Grating-lobe Suppression through Angular Weighting for Laser Induced Phased Arrays

Peter Lukacs
Department of Electronic and Electrical Engineering
University of Strathclyde
Glasgow, UK
peter.lukacs@strath.ac.uk

Don Pieris
Department of Electronic and Electrical Engineering
University of Strathclyde
Glasgow, UK
don.pieris@strath.ac.uk

Geo Davis
Department of Electronic and Electrical Engineering
University of Strathclyde
Glasgow, UK
geo.davis@strath.ac.uk

Paul Wilcox
Department of Mechanical Engineering
University of Bristol
Bristol, UK
p.wilcox@bristol.ac.uk

Theodosia Stratoudaki
Department of Electronic and Electrical Engineering
University of Strathclyde
Glasgow, UK
t.stratoudaki@strath.ac.uk

***Abstract*— Laser Induced Phased Arrays (LIPAs) use lasers to generate and detect ultrasound, synthesizing the array in post processing. Data acquisition is done remotely, without couplant, addressing NDE challenges of inspection on complex structures and under extreme environments. Previously high-resolution ultrasonic imaging of components using LIPAs have been demonstrated by capturing the Full Matrix and employing the Total Focusing Method (TFM) as imaging algorithm. However, the Full Matrix Capture data acquisition method requires long acquisition time due to the mechanical scanning of lasers, compromising the application potential of LIPAs. It is possible to increase the data acquisition speed by reducing the number of array elements. Nevertheless, this can lead to the generation of grating lobes (GL), when the Nyquist sampling limit is exceeded for the interelement spacing of the array. In transducer phased arrays, GL can be suppressed by applying an angular limit in the TFM algorithm. This implementation is ideal for omnidirectional directivity centered around the surface normal, which is not the case for LIPA elements. In this work we are using an adaptive angular weighting factor that is suitable for LIPAs considering LU characteristics.**

Keywords—Laser Ultrasound, Ultrasonic Phased Arrays, Grating Lobe Suppression, Laser Induced Phased Arrays, Synthetic Array Imaging

I. INTRODUCTION

Ultrasonic imaging is an invaluable tool widely used in various fields, such as medicine or non-destructive testing. Conventionally, transducer-based phased arrays are utilised to from ultrasonic images of the test subjects, however, in various applications, their employment can be challenging, such as in extreme environments or in places of restricted access.

Laser Induced Phased Arrays (LIPAs) is a synthetic array technique that utilises one laser for the generation and another for the detection of ultrasonic waves [1]. This technique is completely non-contact, enabling remote sensing, it has a small footprint, can be coupled via optic fibres and can adapt to any complex surface shapes. Coupling the LIPA modality with the Full Matrix Capture (FMC) data acquisition method and using a delay-and-sum imaging algorithm, such as the Total Focusing Method (TFM) has shown to produce significantly higher quality images, compared to previous laser ultrasonic imaging approaches, such as the Synthetic Aperture Focusing Technique (SAFT) [1]. LIPA expand the capabilities of laser ultrasonic arrays for advanced evaluation of the imaged subjects, such as analysis of scattering at varying generation and detection angles [2]. LIPAs can also be realised in 2D configuration towards producing volumetric images [3]. These advantages are afforded by the FMC data acquisition method, which acquires a signal for each generation and detection element combination [4].

However, one challenge of utilising LIPAs is the long data acquisition time required to mechanically scan the generation and detection lasers, independently of each other, to every array element position as opposed to the electronic sweep of transducer array elements in conventional phased arrays. In order to avoid grating lobe artefacts, the interelement spacing of the array must be equal to or less than half the acoustic wavelength. Grating lobe suppression through optimised array design has been presented for LIPAs. Vernier and random 2D array layouts were designed for LIPAs, which were experimentally realised through a 2D scanning system [6].

A possible method for suppressing grating lobe artefacts is through cross-correlating the directivity of laser generated and detected ultrasound with the acquired signals [5]. This method utilises a power factor, which has to be carefully tuned for every array configuration and test subject it is applied on. The disadvantage of this method is that when this power factor is not optimised, the non-linearity introduced by this method can be overwhelming or the grating lobe suppression might not be sufficient. In addition, this method assumes that only idealistic point-scatterers will be present in the test subject. Unfortunately, this is not true for many practical imaging scenarios, where defects may have arbitrary and asymmetrical size, scattering the ultrasound in unpredictable directions.

In this work we are proposing the adaption of an angular weighting in order to suppress grating lobe artefacts, based on the work presented in [7]. The proposed method works well in suppressing grating lobe artefacts but the effect of the angular weighting consequently reduces the angular aperture, which is the range of angles a pixel is viewed from. The downside of reduced angular aperture is a decline in lateral resolution. In order to overcome the adverse effects of the angular weighting, the weighted image is combined with the non-weighted image, such that the final image inherits the absence of grating lobe artefacts from the former and the

The work presented in this paper was supported by the UK Engineering and Physical Sciences Research Council [Grant reference EP/T012862/1, EP/R513349/1, EP/V051814/1].

lateral resolution from the latter. The potential of the method is experimentally demonstrated on a dataset acquired from an aluminium test subject with intentionally induced cylindrical side-drilled defects.

II. Methodology

A. Laser Induced Phased Array

LIPAs acquire a signal for each generation and detection element combination, thus all the possible information is captured for a given array. The signals are combined in post-processing using the TFM algorithm to focus and steer the ultrasonic waves synthetically. The images are produced using

$$I(x,z) = \left|\sum\sum S_{tx,rx}(\tau(x,z))\right|, \quad (1)$$

where

$$\tau(x,z) = \frac{d_{rx}(x,z)+d_{tx}(x,z)}{c}, \quad (2)$$

$S_{tx,rx}$ is the signals captured using generation element *tx*, and detection element *rx*, $d_{tx}(x,z)$ is the distance between generation element tx and pixel at (x,z), $d_{rx}(x,z)$ is the distance between pixel at (x,z) and the detection element and c is the acoustic wave velocity.

When the pitch of an array is larger than half the acoustic wavelength, grating lobes appear during focusing, at angles other than the angle of the main lobe, which leads to the appearance of undesirable artefacts.

B. Grating Lobe Suppression through Angular Weighting

Fig. 1 shows example TFM images when processing different portions of the full matrix dataset, in order to provide a visual demonstration of how grating lobe artefacts affect LIPA imaging.

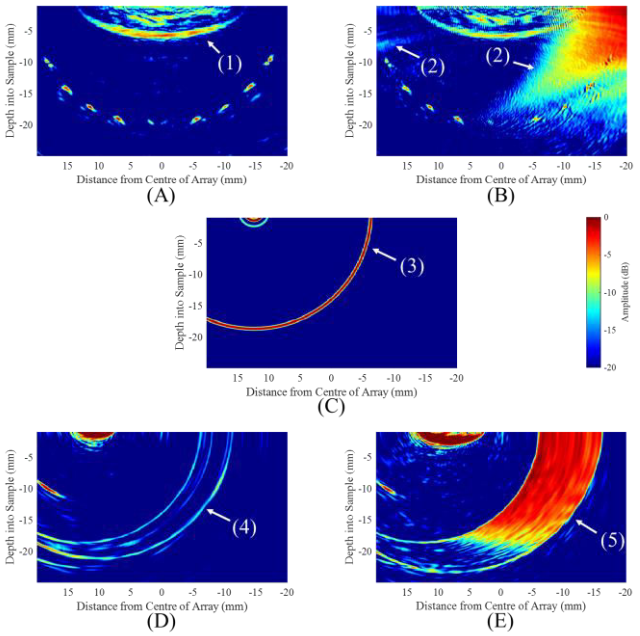

Fig. 1. A) and B) TFM images of a sample with 9 defects using A) λ/2 and B) λ pitch, with the same total aperture, C) contribution of a single A-scan. D) and E) Two images are produced by selecting a single generation and 80 detection points with D) λ/2 and E) λ pitch. Colorbar indicates the dynamic range of all images within the figure.

Images shown in Fig. 1 A) and B) were produced using a dense (λ/2 pitch) and a sparse (λ pitch) equidistant array, respectively. Each image shows the surface acoustic wave (SAW) cross-talk region [1] (arrow (1)). They will be ignored for this study, as they are unrelated to grating lobes. The effect of grating lobes (arrow (2)) can be clearly seen on B), especially on the artefacts present at the right-hand side of the TFM image. These artefacts are not present on A), as expected because the dataset for this image was captured using a dense array. Fig. 1 C) shows the contribution of a single A-scan signal on the TFM image, in order to demonstrate how these artefacts are produced. The most noticeable feature on this image is a large red arc (arrow (3)), which is produced by the reflection of the SAW from the edge of the sample. SAWs are generated at the same time as the bulk ultrasonic waves during laser ultrasonic generation and are considerably higher amplitude than bulk waves, thus the SAW can appear at high amplitudes on the TFM images.

When multiple A-scan signals are added up using the TFM algorithm, the SAW will be coherent only at the surface of the sample, thus its contribution within the bulk will be cancelled out. This is demonstrated in Fig 1 D) where the arcs produced by the SAW are destructively interfering with each other, resulting in a lower amplitude of these features (arrow (4)). Some residue of the SAW is still present on Fig 1 D), which can be explained by the following: 1) the statement that SAWs are only coherent at the surface assumes that the image processing uses the SAW instead of the bulk velocity, which is not true in this case, thus focusing of the SAWs will be inaccurate, 2) only an infinitely long array would be capable of fully eliminating grating lobes.

When the array is sparse, SAWs are not destructively interfering, due to the spatial under sampling. This is demonstrated on Fig. 1 E), where the same number of signals were utilised as in Fig 1 D), captured in this case with a sparse array. In contrast to the image produced by the dense array, the contribution of the SAW reflections appears at significantly higher amplitude (arrow (5)), due to the effect of the grating lobes produced by the sparse array.

Defining the angles that signals can contribute at is expected to limit the impact of grating lobes. In this work these angles are defined as a weighting, based on the laser ultrasonic generation and detection directivities [7]. Only limited information can be acquired at angles where the laser generation or detection directivity is low, thus, summing the signals at these angles can only provide signals from grating lobes and noise. The weighting ensures that signals are only summed at angles where echoes can originate from. The laser ultrasonic directivities are dependent on the acoustic properties of the material that ultrasound is generated and detected in [1]. Example generation and detection directivities are shown on Fig 2, using the acoustic properties of aluminium. The generation (G) and detection (D) directivities are described in detail in [1].

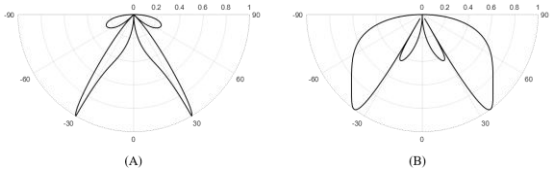

Fig. 2. Laser ultrasonic shear (A) genearion and (B) detection directivities for aluminium. Amplitude axes are normalised to the maximum directivity respectively.

The directivities are applied, as described in [7], by

$$I_w(x,z) = \left|\sum\sum G_{tx}(x,z)D_{rx}(x,z)S_{tx,rx}\left(\tau(x,z)\right)\right|. \quad (3)$$

where $G_{tx}(x,z)$ and $D_{rx}(x,z)$ are the generation and detection directivities for the angle between the generation element *tx* and point *(x,z)* and detection element *rx* and point *(x,z)*, respectively. In order to demonstrate the effect of the angular weighting, Fig 1. C) and E) were reprocessed using (3). The original, unweighted images can be seen on Fig. 3 A) and C), while the images produced after applying the weighting can be seen on B) and D), respectively.

In the case of using a single A-scan signal, shown in Fig. 3 A) and B), it can be seen that the angular weighting considerably limits the contribution of the SAW reflection, to the only positions that ultrasonic (bulk) echoes can originate from. Consequently, this has a large impact when multiple A-scans are utilised in the post-processing algorithm. The SAW reflections are now constrained to small regions of the image, as shown on Fig. 3 B), thus they no longer overlap with each other. This leads to a considerable suppression of the artefacts, as shown on Fig. 3 C) and D).

C. *Restoring Lateral Resolution*

Lateral resolution of an ultrasonic phased array is defined by the aperture. A large aperture can inspect the bulk of the sample from a wider range of angles, and this range, the angular aperture then translates to high lateral resolution. The methodology defined in Section II. B suppresses grating lobe artefacts by limiting the contribution of signals at a wide range of angles in the imaging domain. This effectively means that the angular aperture is reduced, thus lateral resolution is expected to deteriorate. In order to recover the lateral resolution a minimisation process is applied between the images obtained by (1) and (3), using

$$I_R(x,z) = min\left(I(x,z)I_w(x,z)\right). \quad (4)$$

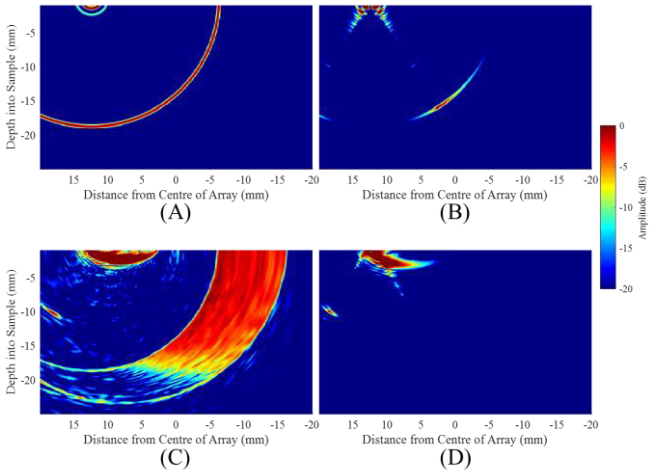

Fig. 3. TFM images of a sample with 9 defects using A,B) a single A-scan signal and C,D) 80 A-scan signals. Images are processed A,C) without and B,D) with angular weighting.

III. Results

A. *Experimental Conditions*

In this study two lasers were utilised, one for generation and one for detection of ultrasound. The former was a Q switched Nd:YAG laser with a pulse width of 8 ns, 300μJ energy per pulse, and a repetition rate of 1 kHz, while the latter was a rough surface interferometer (Quartet, Sound & Bright) with 780mW power, operating in continuous wave mode. The generation laser was focused onto a line, while the detection laser was focused onto a spot. The scanning of the laser beams on the inspection surface was done by a galvo-scanning mirror for the former and, a motorised linear stage for the latter.

The experiment was carried out on an aluminium block with 9 cylindrical side-drilled holes, with 1 mm diameter, located in an arc, as shown on Fig. 4. The two lasers were scanned independently of each other on the inspection side (same side generation and detection of ultrasound) in order to capture the Full Matrix. The synthetic array had 81 array elements, thus a total of 6561 A-scan signals were acquired. The interelement spacing was 0.31 mm. In post-processing a Gaussian digital filter was applied to each A-scan signal individually, with a centre frequency of 5 MHz and a -6 dB bandwidth of 10 MHz. An analogue high pass filter of 1 MHz was used in ultrasonic detection, thus the effective frequency range available after filtering was 1-10 MHz. The acoustic wavelength calculated for the highest frequency component (i.e. 10 MHz) was 0.31 mm, thus at this frequency the pitch was equal to 1λ, making this array sparse.

B. *Imaging Results*

The experimental imaging results can be seen on Fig. 5. Imaging without and with the angular weighting can be seen on Fig. 5 A) and B), respectively. The combination of the two images, achieved through minimisation, as per (4), can be seen on Fig. 5 C). Grating lobe artefacts appear on the image without angular weighting, making the interpretation of the image challenging, thus it is hard to located and identify the defects. After applying the angular weighting on the image, the grating lobe artefacts are considerably suppressed, as shown on Fig. 5 B).

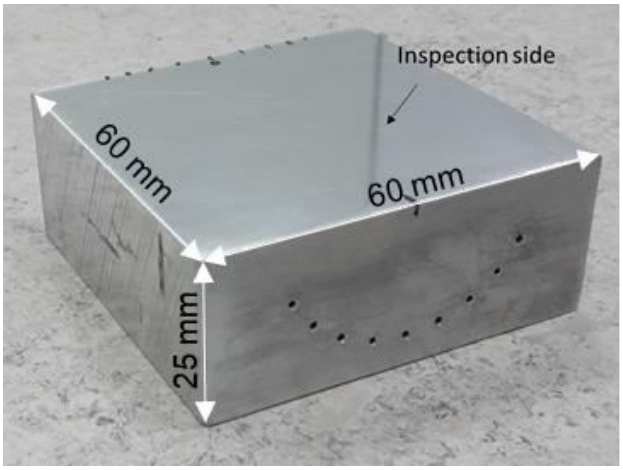

Fig. 4. Experimental test sample, showing the inspection side and the 9 cylindrical side-drileld holes.

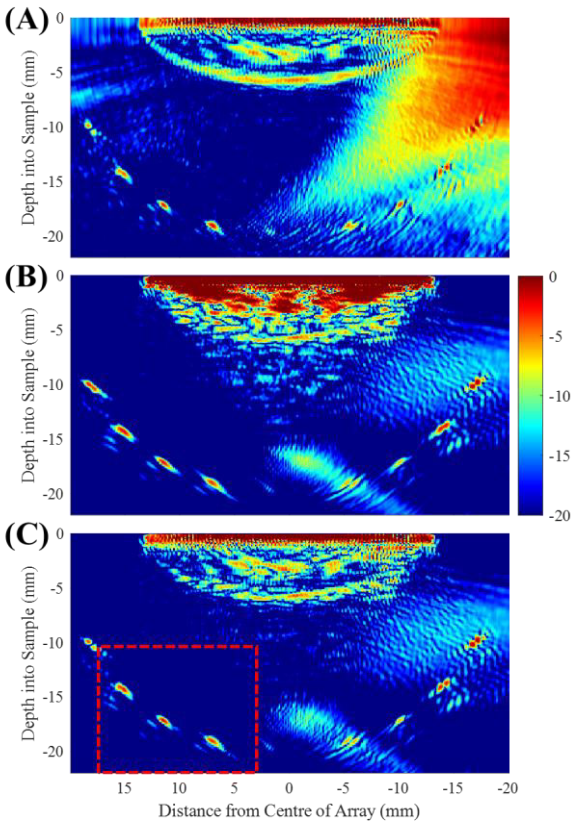

Fig. 5. Experimental ultrasonic images A) without angular weighting, B) with angular weighting and C) the combination of the two through minimisation. Red dashed box indicated location of close-up images shown in Fig. 6.

After the weighting is applied the defect indications appear enlarged compared to the image produced with no weighting (Fig. 5 A) and B)), as expected. The lateral resolution is recovered after the two images were combined through minimisation, while the grating lobe artefact suppression is maintained (Fig. 5 C)).

In order to evaluate the size of the defect indications the amplitude of the images is extracted along the red dashed line highlighted on Fig. 6 B). The amplitudes measured on the three images, along the red dashed line, are shown on Fig. 7.

The graph on Fig 7 confirms that the defect indication on the weighted image is larger than without the weighting. The -6 dB drop, relative to their independent peaks, were 1.56 mm and 1.02 mm for the weighted and the combined image through minimisation, respectively. The sizing error was 56% when the weighting was used, relative to the true size of the defect (1 mm) while after the minimisation the error was reduced to 2%.

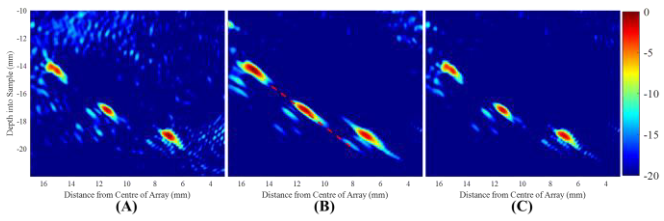

Fig. 6. Close-up of three defect from figure 5 (red dashed box), A) without angular weighting, B) with angular weighting and C) the combination of the two. Red dashed line on B) indicates the positions at which defect sizing was carried out.

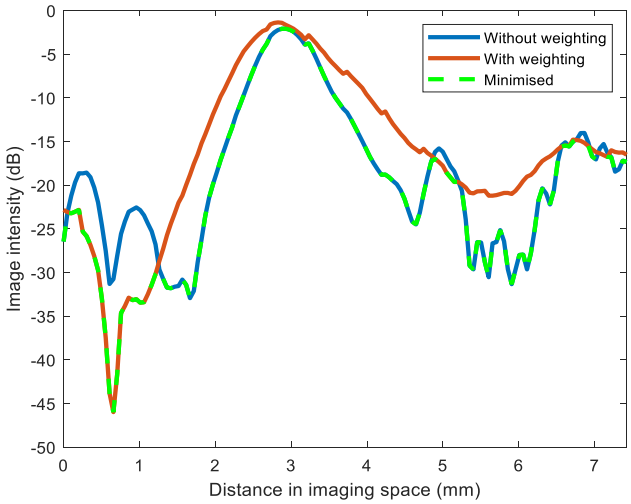

Fig. 7. Amplitude of three images from Fig. 6, across the red dashed line highlighted on Fig. 6 B).

IV. CONCLUSION

Angular weighting based on the laser ultrasonic generation and detection directivities for grating lobe suppression was presented in this work. The weighting limits the contribution of grating lobes at a wide range of angles, while maintaining the amplitude of signals from the angles they originated from. It was demonstrated that while applying such angular weighting can suppress grating lobes, it adversely impacts lateral resolution. In order to maintain the grating lobe suppression achieved through the angular weighting, and maintain the lateral resolution without angular weighting, a process of minimisation of the two images was introduced. Defect sizing was carried out for a 1 mm diameter cylindrical defect. Measuring the width of the defect indication at the -6 dB from its peak, the sizing error was reduced by 54% after applying minimisation.

REFERENCES

[1] T. Stratoudaki, M. Clark, and P. D. Wilcox, “Laser induced ultrasonic phased array using full matrix capture data acquisition and total focusing method,” Opt. Express, vol. 24, no. 19, pp. 21921, 2016.

[2] K. Tant, and T. Stratoudaki, "Reconstruction of Missing Ultrasonic Phased Array Data Using Matrix Completion." IEEE Int. Ultrason. Symp., pp. 627-630, 2019.

[3] P. Lukacs, G. Davis, T. Stratoudaki, Y. Javadi, G. Pierce, and A. Gachagan, “Remote, volumetric ultrasonic imaging of defects using two-dimensional laser induced phased arrays,” in Quantitative Nondestructive Evaluation, vol. 85529, p. V001T18A001, American Society of Mechanical Engineers, 2021.

[4] C. Holmes, B. W. Drinkwater, and P. D. Wilcox, “Post-processing of the full matrix of ultrasonic transmitreceive array data for non-destructive evaluation,” NDT E Int., vol. 38, no. 8, pp. 701–711, 2005.

[5] H. He, K. Sun, C. Sun, J. He, E. Liang, and Q. Liu. "Suppressing artifacts in the total focusing method using the directivity of laser ultrasound." Photoacoustics, 31, 2023.

[6] P. Lukacs, G. Davis, D. Pieris, A. Gachagan, and T. Stratoudaki. "Grating Lobe Suppression Through Novel, Sparse Laser Induced Phased Array Design." IEEE Int. Ultrason. Symp., pp. 1-4., 2022.

[7] T. Stratoudaki, M. Clark, and P. Wilcox. "Adapting the full matrix capture and the total focusing method to laser ultrasonics for remote non destructive testing." IEEE Int. Ultrason. Symp., pp. 1-4., 2017.